Resonance-driven heat transfer enhancement in a natural convection boundary layer perturbed by a moderate impinging jet

Naoto Ogasawara [1,2,*] Juan F. Torres [3,*] Yuki Kanda [2]
Takuma Kogawa [4] and Atsuki Komiya [2]

[1] *School of Engineering, Tohoku University, Aramaki, Aoba-ku, Sendai 980-8579, Japan*
[2] *Institute of Fluid Science, Tohoku University, Katahira, Aoba-ku, Sendai 980-8577, Japan*
[3] *School of Engineering, Australian National University, Canberra, ACT 2601, Australia*
[4] *National Institute of Technology Hachinohe College, Uwanotai, Tamonoki, Hachinohe 039-1192, Japan*

We report a resonance-driven convective heat transfer enhancement downstream of a natural convection boundary layer that is perturbed by a moderate impinging jet. Flow resonance is experimentally and numerically confirmed between the boundary layer and a periodic flow driven by the unbalance of jet momentum and buoyancy. When the oscillation frequency in the impinging region is a submultiple of the characteristic frequency of natural convection, downstream heat transfer enhancement E from the baseline of natural convection exceeds 40%. In contrast, further increasing the jet momentum fourfold yields $E < 20\%$. The results support the development of efficient heat transfer enhancement methods.

Natural convection is a ubiquitous heat and mass transfer phenomenon where a nonisothermal fluid flow is spontaneously generated due to density differences under a gravitational field. Beyond its fundamental importance, natural convection has a wide range of engineering applications, e.g., in cooling towers and nuclear waste, because heat transfer significantly increases with the spatial scale [1,2]. Importantly, natural convection cooling is a low-energy consumption heat transfer mechanism due to its passive nature, in contrast with active cooling methods that purely rely on forced convection, e.g., using a fan. Convective cooling can be further amplified by fin arrays [3,4], but their implementation in large surfaces is challenging due to manufacturing costs and potential reduction in heat transfer for mixed convection regimes where hot air is trapped between the fins [4].

If natural convection by itself is not sufficient for cooling, then low-energy active methods for enhancing heat transfer become essential, such as introducing a disturbance using a vibrating ribbon near the leading edge [5], injecting millimeter-sized bubbles in a two-phase flow [6], and controlling natural convection by a freestream [7], oblique [8], or directly impinging jet [9]. Directly impinging jets at high Reynolds numbers enhance heat transfer near the impinging region, but not necessarily on a large surface area, besides requiring a larger power consumption than moderate flow jets. In addition, an active control method was recently proposed based on numerical simulations whereby heat transfer is enhanced due to a resonance effect that occurs between the characteristic frequency of a natural convection boundary layer and that of the imposed perturbation (fluctuating wall temperature) near the leading edge [10]. On the other hand, a mixed convection region, such as that of a jet impinging on a natural convection boundary layer, is expected to yield oscillating
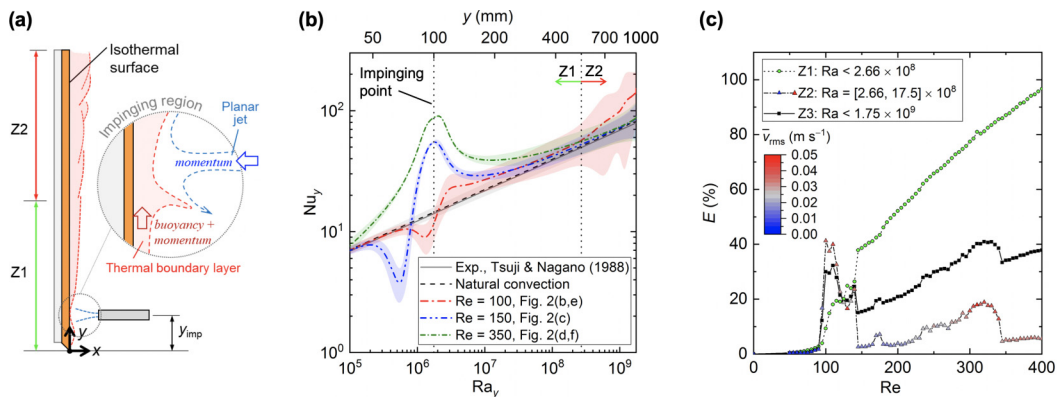
---

*These authors contributed equally to this work.

FIG. 1. Heat transfer enhancement of natural convection ($Ra_y < 1.75 \times 10^9$) by an impinging planar jet ($Re < 400$). (a) Schematic of the physical problem, consisting of natural convection from an isothermal vertical wall on which the jet impinges near the leading edge. The inset focuses on the impinging region where the unbalanced forces of buoyancy and momentum can cause flow instability. (b) Nu_y as a function of Ra_y for natural convection and three jet Re. (c) Dependence of heat transfer enhancement E on Re in two regions: zone 1 (Z1) for $Ra_y < 2.66 \times 10^8$, and zone 2 (Z2) for $Ra_y = 2.66 \times 10^8$ to 1.75×10^9; zone 3 (Z3) comprises both zones. The large E at moderate Re and its associated cause (resonance) is the main focus of this study. The color bar shows the rms velocity probed at $y = 700$ mm.

flows when the buoyancy (stabilizing) and externally imposed momentum (destabilizing) have a similar magnitude [11]. Here, we explore the possibility of using such a perturbing oscillating flow produced by a local mixed convection regime to subsequently trigger flow resonance downstream of a natural convection boundary layer, enhancing heat transfer. Furthermore, if the heat transfer enhancement due to the impinging jet and downstream flow resonance can be combined, then a low-energy method for enhancing convective heat transfer may be achieved.

To evaluate the proposed method of heat transfer enhancement by a moderate impinging jet applying flow resonance, we focus on natural convection with Rayleigh number up to $Ra_y = 1.75 \times 10^9$ and jet flow with Reynolds number up to $Re = 400$ (see Note 1 in the Supplemental Material [12]). A schematic of the system is shown in Fig. 1(a), with a focus on the impinging region where a local mixed convection regime occurs. We visualized the thermal boundary layer with a large-aperture interferometric technique [13–17] validated here against a well-known experimental benchmark [18] (Fig. S1, Supplemental Material [12]). In addition, to quantitatively evaluate the heat transfer enhancement, we carried out numerical simulations (Fig. S2) using a large eddy simulation (LES) model [19,20] previously validated against experimental results [21,22] (Supplemental Material Note 2). Transient numerical simulations were conducted for 300 s, enough time to obtain a fully developed flow. Both experiments and simulations are performed for a vertical heated plate with a height of 1000 mm and wall temperature of 316 K, while the jet and ambient temperature is 296 K. A planar jet impinged onto the isothermal surface at $y_{imp} = 100$ mm ($Ra_y = 1.75 \times 10^6$), with the distance between the nozzle and impinged surface 50 mm, and a nozzle height of 10 mm. u_{jet} was uniform on the jet outlet in the simulation and experimentally measured at the jet central plane within the potential core [23] (Fig. S3). Experimentally, the field of view was 120 mm, and the plate was displaced vertically to capture the thermal boundary layer throughout the entire plate length. The vertical heated plate was 150 mm wide, made of aluminum alloy, and controlled by a PID system. The planar jet nozzle was 10 mm high, 220 mm wide, and 300 mm long; its flow rate was adjusted with a compressor and valves (Fig. S4). A turbulence intensity of up to 2% was obtained experimentally, which can have a marginal effect on the heat transfer [23,24].

Figure 1(b) plots the local Nusselt number $Nu_y = h_y y/k$ as a function of Ra_y obtained by simulations; h_y and k are the local heat transfer coefficient and thermal conductivity of air. The

results for natural convection yielded a good agreement with the empirical correlation of laminar natural convection [18]. For the impinging jet at moderate flow rate such as Re = 100 and 150, Nu_y decreased below the impinging point $Ra_y(y_{imp})$ due to the opposing buoyancy and externally induced momentum, whereas it increased above $Ra_y(y_{imp})$ due to their assisting configuration. Ra_y corresponding to the peak of Nu_y approached $Ra_y(y_{imp})$ as Re was increased. When Re = 350, Nu_y behaved as a wedge flow [25], since forced convection was much stronger than natural convection. The shaded area represents the standard deviation of the simulated time series. The largest time variation of Nu_y was confirmed at Re = 100. Interestingly, for jets of Re = 100, Nu_y drastically increased for $y > 533$ mm ($Ra_y = 2.66 \times 10^8$) compared to the other conditions, which is due to a peculiar flow interaction that we further elucidate.

The heat transfer enhancement from the baseline case of natural convection, which is defined as E, is expected to have different characteristics around y_{imp} and for $y > 533$ mm. Therefore, we divided the evaluation region into two zones as shown in Fig. 1(a): zone 1 (Z1) for $Ra_y < 2.66 \times 10^8$ and zone 2 (Z2) between $Ra_y = 2.66 \times 10^8$ and 1.75×10^9. Zone 3 (Z3) encompassed the entire plate. The zones were determined by the threshold at which local heat transfer begins to increase when Re = 100 (Fig. S5), and are fixed for all Re. E is defined as $E = (\overline{Nu_{imp}} - \overline{Nu_n}) \times 100/\overline{Nu_n}$, where $\overline{Nu_{imp}}$ and $\overline{Nu_n}$ are the spatial average of Nu_y in each zone for the cases of impinging jet and pure natural convection.

Figure 1(c) shows the dependence of E on the jet Re for each zone. For all conditions, the jet increased E. Interestingly, E monotonically increased in Z1 for all Re, but in Z2 it increased to approximately 40% for Re = 100 while decreasing to approximately 2.7% and 5.2% for Re = 150 and 350, respectively. These results demonstrate that the heat transfer was enhanced not only in a zone that encompasses the impinging region (Z1), but also downstream of the thermal boundary layer (Z2), in particular for a moderate Re. The color bar plotted on the markers for the results of Z2 shows the root mean square (rms) of the y component of velocity probed at $y = 700$ mm, averaged in the x direction. Even though the rms velocity at Re = 100 has equivalent values as Re > 300, E for the former was more than twice the latter. This suggests that the large E at Re = 100 is caused by factors other than a large rms velocity. We investigate the existence of flow resonance as a possible explanation for such a dramatic increase in E, i.e., resonance between the downstream natural convection boundary layer and perturbations produced by the oscillating flow in the impinging region.

The first aim of the numerical simulations was to visualize the temperature field over the heated surface to clarify the mechanism of the heat transfer enhancement. Figures 2(a)–2(d) show the instantaneous temperature field for the entire calculation domain. Large instability waves of the thermal boundary layer over Z2 are clearly observed for Re = 100, but not Re = 150 and 350 (wedge flow). These results suggest that the instability waves are responsible for the large E when Re = 100, and its further reduction at Re = 150 and 350, as reported in Fig. 1(c) and Video S1 (Supplemental Material [12]).

Figures 2(e) and 2(f) show a good qualitative agreement between the instantaneous temperature fields in the impinging region obtained by the simulations and visualization experiments. In Fig. 2(e) when Re = 100, the buoyancy assisting region and buoyancy opposing region are confirmed as reported in [26]. In Fig. 2(f) when Re = 350, the thermal boundary layer was confirmed to have a wedge flow shape. These visualization results support the heat transfer mechanism at the impinging point as discussed in relation to Fig. 1(b). The periodic perturbation of the thermal boundary layer caused by the unbalanced forces of buoyancy and momentum was observed when Re = 100. Video S2 shows the thermal boundary layer instability in the impinging region, and downstream at $y = 400, 700$ mm, while perturbed by a jet of varying Re.

The periodicity of these fluctuations at the impinging point is thought to have introduced the resonance of the thermal boundary layer downstream. According to Zhao *et al.* [10], the characteristic frequency of the natural convection thermal boundary layer (f_c) is 1.68 Hz under the present conditions with $\Delta T = 20$ K. It can be considered that the significant large E for Re = 100 was
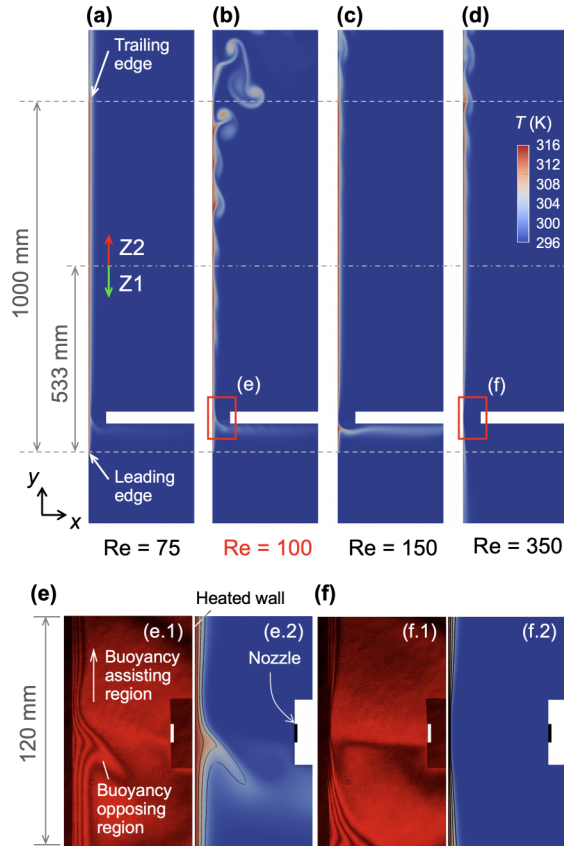
FIG. 2. Visualized instantaneous temperature fields after 300 s from the start of impinging jet. Numerical results over the entire heated wall for (a) Re = 75, (b) Re = 100, (c) Re = 150, (d) Re = 350. Instability waves of the thermal boundary layer over the heated surface were observed for Re = 100 (also moderately at Re = 250 in Video S1). The comparison between experiments (red interferograms) and simulations around the impinging region are shown in (e) when Re = 100, and (f) Re = 350 (Video S2 shows more comparisons).

caused by the resonance effect of natural convection if the temperature fluctuations in the boundary layer occur close to the characteristic frequency or submultiples of the characteristic frequency when Re = 100. Therefore, we first performed fast Fourier transform (FFT) of the numerical simulation results and the experimental results for Re = 100 to assess whether the natural convection resonance effect occurred. The FFT analysis in the simulations was conducted by processing the temperature time variations at three points ($x = 2\,\text{mm}$, $y = 130, 400$, and $700\,\text{mm}$). In the experiment, the FFT was performed by processing the visualized temperature field. We measured the time fluctuations of the external position of the interference fringes, which is approximately the boundary layer thickness, at the same height as the numerical simulations (Video S3), and then obtained the corresponding power spectra. FFT was performed on the simulation results for 100 s and the experimental results for 30 s using Hanning window function. We confirmed that the sampling periods did not significantly affect the FFT results.

Regarding the simulation results of the temperature time series for Re = 100, the periodic temperature perturbation was found across the entire wall, as shown in Fig. 3(a) at three spread locations. This indicates that the thermal boundary layer does not become turbulent within the simulated length despite the observed instability waves in Fig. 2(b). In addition, the amplitude of the temperature fluctuations increased streamwise of the natural convection flow. In
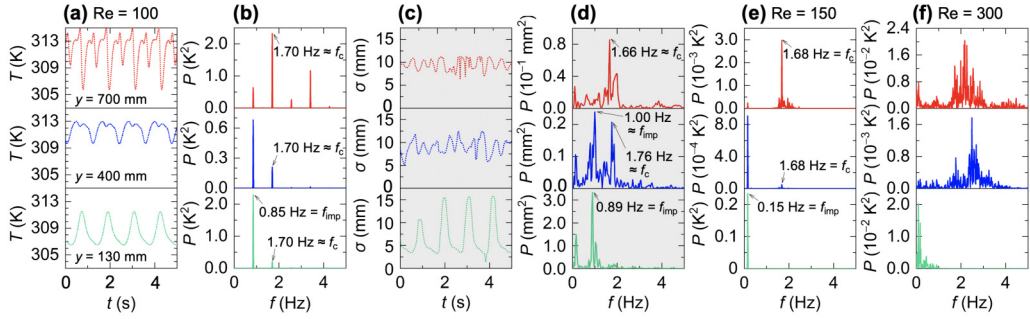
FIG. 3. Thermal boundary layer analysis at three different locations: $x = 2$ mm and $y = 130$ mm (bottom/green), 400 mm (middle/blue), and 700 mm (top/red). Numerical simulation results showing the temperature time series (a) and power spectra (b) for Re = 100. Experimental results (gray background) for thermal boundary layer fluctuations (c) and power spectra (d) for Re = 100 at the same locations. Simulation results showing the power spectra for Re = 150 (e) and Re = 300 (f); Fig. S8 shows the temperature time series. The dotted (a),(c) and solid (b),(d)–(f) lines represent probed values and power spectra, respectively.

particular, the large amplitude is confirmed at $y = 700$ mm (Z2). Figure 3(b) show the corresponding power spectra at each position for Re = 100. A frequency component of 1.70 Hz that is close to the natural frequency $f_c = 1.68$ Hz of the natural convection boundary layer [10] was identified. The intensity at 1.70 Hz increased along the streamwise direction, while the component of the impinging point $f_{imp} = 0.85$ Hz decreased. This phenomenon suggests the existence of resonance between the flow having a frequency f_c and f_{imp}. An interesting point is that while the peak frequency at the impinging location was $f_{imp} = 0.85$ Hz, a frequency component with integer multiple of f_{imp} appears downstream, such as 1.70, 2.56, 3.41 Hz (Fig. S6). This change of the peak frequencies with the location along the heated surface was also observed by Zhao *et al.* [27]. In addition, this change can be characterized as harmonics of the fundamental wave with frequency 0.85 Hz, which is reported in another natural convection resonance study [28,29]. Therefore, the periodic temperature fluctuations due to the instability of the mixed convection at the impinging point become the fundamental wave of harmonics, inducing perturbations with the characteristic frequency of natural convection that leads to flow resonance. The temperature amplitude increase could be attributed to the resonance effect, leading to a strong fluctuation of the thermal boundary layer that in turn results in a much larger E when Re = 100 than the case of Re > 150.

Regarding the transient measurement of the thermal boundary layer thickness σ, its periodic fluctuation frequencies agreed well with numerical predictions, in particular at $y = 130$ mm. Although well-defined periodic patterns were not clearly observed at $y = 400$ and 700 mm in Fig. 3(c), the power spectra in Fig. 3(d) matched very well with the numerical results in Fig. 3(b) despite having different probes. The resonance effect was then thought to be experimentally confirmed since the frequency components close to the characteristic frequency increased in the y direction, while the components of the frequency at the impinging point decreased. In addition to the evaluation of the thermal boundary layer thickness, we also experimentally confirmed the resonance effects by FFT of the temperature time series obtained by a thermocouple (Fig. S7). In order to further test the hypothesis of flow resonance, the same analysis was repeated for larger Re.

Figures 3(e) and 3(f) indicate that the power spectra obtained by simulations when Re = 150 and 300 lacked flow resonance. In the case of Re = 150 [Fig. 3(e)], the peak frequency in the impinging region was 0.15 Hz while at $y = 400$ and 700 mm significantly weak peak frequencies were obtained (note the units). This is because the frequency at the impinging region is far from the fundamental wave of the harmonics 0.84 Hz (as observed for Re = 100). The weak peaks at the natural convection natural frequency 1.68 Hz at $y = 700$ mm are thought to occur because of a frequency filtering of natural convection, and not caused by resonance effect [30,31]. As Re was

further increased to Re = 300 [Fig. 3(f)], the power spectrum had random peak frequencies since the temperature variation became nonlinear over the heated surface [Fig. S8(b)]. The randomness of this flow regime was also experimentally confirmed by the interferometric measurement of the thermal boundary layer (Fig. S9, Video S3).

In conclusion, we show the existence of a peculiar heat transfer enhancement mode downstream of a natural convection boundary layer caused by flow resonance between (a) a periodic perturbation caused by a moderate jet impinging onto the upstream natural convection boundary layer, and (b) the characteristic frequency of the natural convection boundary layer. For Re = 100, instability waves were observed over the heated surface, and the downstream heat transfer enhanced about 40% from pure natural convection. It was hypothesized, and then confirmed by numerical simulations and experimental observations, that the large E was caused by flow resonance. The resonance effect is induced when the thermal boundary layer at the impinging point fluctuates at a frequency of half the natural convection characteristic frequency, which causes harmonics to occur. Combining flow resonance (downstream) and thinning of the boundary layer by the impinging jet (upstream) provides a powerful means of further enhancing heat transfer. The results present physical insight into the mechanisms of flow resonance in mixed convection flows and encourage the development of new low-power consumption heating and cooling methods.

[1] M. D. Su, G. F. Tang, and S. Fu, Numerical simulation of fluid flow and thermal performance of a dry-cooling tower under cross wind condition, J. Wind Eng. Ind. Aerodyn. **79**, 289 (1999).

[2] X. Heng, G. Zuying, and Z. Zhiwei, A numerical investigation of natural convection heat transfer in horizontal spent-fuel storage cask, Nucl. Eng. Des. **213**, 59 (2002).

[3] T. Aihara, S. Maruyama, and S. Kobayakawa, Free convective/radiative heat transfer from pin-fin arrays with a vertical base plate (general representation of heat transfer performance), Int. J. Heat Mass Transfer **33**, 1223 (1990).

[4] J. F. Torres, F. Ghanadi, Y. Wang, M. Arjomandi, and J. Pye, Mixed convection and radiation from an isothermal bladed structure, Int. J. Heat Mass Transfer **147**, 118906 (2020).

[5] Y. Jaluria and B. Gebhart, An experimental study of nonlinear disturbance behaviour in natural convection, J. Fluid Mech. **61**, 337 (1973).

[6] A. Kitagawa, P. Denissenko, and Y. Murai, Effect of heated wall inclination on natural convection heat transfer in water with near-wall injection of millimeter-sized bubbles, Int. J. Heat Mass Transfer **113**, 1200 (2017).

[7] K. Kitamura, M. Yamamoto, and F. Kimura, Fluid flow and heat transfer of opposing mixed convection adjacent to vertical heated plates, Heat Transfer - Asian Res. **34**, 595 (2005).

[8] R. Mondal, J. F. Torres, G. Hughes, and J. Pye, Analysis of air curtains for natural convection heat-loss mitigation, in *Proceedings of the 22nd Australasian Fluid Mechanics Conference (AFMC)*, edited by H. Chanson and R. Brown (The University of Queensland, Brisbane, Australia, 2020).

[9] K. Habibi, S. Amiri, and M. Ashjaee, Study of mixed convection characteristics of confined planar jet impingement using the direct temperature gradient interferometric method, Int. J. Therm. Sci. **71**, 205 (2013).

[10] Y. Zhao, P. Zhao, Y. Liu, Y. Xu, and J. F. Torres, On the selection of perturbations for thermal boundary layer control, Phys. Fluids **31**, 104102 (2019).

[11] K. Wu, B. D. Welfert, and J. M. Lopez, Complex dynamics in a stratified lid-driven square cavity flow, J. Fluid Mech. **855**, 43 (2018).

[12] See Supplemental Material at http://link.aps.org/supplemental/10.1103/PhysRevFluids.6.L061501, which includes Refs. [32,33], for details of the numerical simulation and experiments.

[13] E. Shoji, A. Komiya, J. Okajima, and S. Maruyama, Development of quasi common path phase-shifting interferometer for measurement of natural convection fields, Int. J. Heat Mass Transfer 55, 7460 (2012).

[14] J. F. Torres, A. Komiya, J. Okajima, and M. Shigenao, Measurement of the molecular mass dependence of the mass diffusion coefficient in protein aqueous solutions, Defect Diffus. Forum (Genova) 326–328, 452 (2012).

[15] J. F. Torres, A. Komiya, E. Shoji, J. Okajima, and S. Maruyama, Development of phase-shifting interferometry for measurement of isothermal diffusion coefficients in binary solutions, Opt. Lasers Eng. 50, 1287 (2012).

[16] T. Kogawa, E. Shoji, J. Okajima, A. Komiya, and S. Maruyama, Experimental evaluation of thermal radiation effects on natural convection with a rayleigh number of 108–109 by using an interferometer, Int. J. Heat Mass Transfer 132, 1239 (2019).

[17] J. F. Torres, Y. Zhao, S. Xu, Z. Li, and A. Komiya, Optical Method for Simultaneous High-Resolution Measurement of Heat and Fluid Flow: The Case of Rayleigh-Bénard Convection, Phys. Rev. Appl. 14, 054038 (2020).

[18] T. Tsuji and Y. Nagano, Characteristics of a turbulent natural convection boundary layer along a vertical flat plate, Int. J. Heat Mass Transfer 31, 1723 (1988).

[19] T. Kogawa, J. Okajima, A. Komiya, S. Armfield, and S. Maruyama, Large eddy simulation of turbulent natural convection between symmetrically heated vertical parallel plates for water, Int. J. Heat Mass Transfer 101, 870 (2016).

[20] T. Kogawa, J. Okajima, A. Sakurai, A. Komiya, and S. Maruyama, Influence of radiation effect on turbulent natural convection in cubic cavity at normal temperature atmospheric gas, Int. J. Heat Mass Transfer 104, 456 (2017).

[21] T. Fujii, M. Takeuchi, M. Fujii, K. Suzaki, and H. Uehara, Experiments on natural-convection heat transfer from the outer surface of a vertical cylinder to liquids, Int. J. Heat Mass Transfer 13, 753 (1970).

[22] T. Tsuji and T. Kajitani, Turbulence characteristics and heat transfer enhancement of a natural convection boundary layer in water along a vertical flat plate, Proc. IHTC 13, 9 (2006).

[23] L. Guyonnaud, C. Solliec, M. Dufresne de Virel, and C. Rey, Design of air curtains used for area confinement in tunnels, Exp. Fluids 28, 377 (2000).

[24] J. F. Torres, F. Ghanadi, I. Nock, M. Arjomandi, and J. Pye, Mixed convection around a tilted cuboid with an isothermal sidewall at moderate reynolds numbers, Int. J. Heat Mass Transfer 119, 418 (2018).

[25] G. K. Batchelor, *An Introduction to Fluid Dynamics* (Cambridge University Press, Cambridge, UK, 2000).

[26] N. Ramachandran, T. S. Chen, and B. F. Armaly, Mixed convection in stagnation flows adjacent to vertical surfaces, J. Heat Transfer 110, 373 (1988).

[27] Y. Zhao, C. Lei, and J. C. Patterson, Resonance of the Thermal boundary layer adjacent to an isothermally heated vertical surface, J. Fluid Mech. 724, 305 (2013).

[28] L. Zhou, S. W. Armfield, N. Williamson, M. P. Kirkpatrick, and W. Lin, Resonance in natural convection flow subjected to time-varying thermal forcing in an air-filled cavity, in *Proceedings of the 21st Australasian Fluid Mechanics Conference (AFMC)*, edited by T. C. W. Lau and R. M. Kelso (Australasian Fluid Mechanics Society, Adelaide, Australia, 2018).

[29] Y. Zhao, C. Lei, and J. C. Patterson, Transition of natural convection boundary layers-a revisit by bicoherence analysis, Int. Commun. Heat Mass Transfer 58, 147 (2014).

[30] M. J. M. Krane and B. Gebhart, The hydrodynamic stability of a one-dimensional transient buoyancy-induced flow, Int. J. Heat Mass Transfer 36, 977 (1993).

[31] B. Gebhart and R. Mahajan, Characteristic disturbance frequency in vertical natural convection flow, Int. J. Heat Mass Transfer 18, 1143 (1975).

[32] A. W. Vreman, An eddy-viscosity subgrid-scale model for turbulent shear flow: algebraic theory and applications, Phys. Fluids 16, 3670 (2004).

[33] G. E. Lau, G. H. Yeoh, V. Timchenko, and J. A. Reizes, Large-eddy simulation of natural convection in an asymmetrically-heated vertical parallel-plate channel: assessment of subgrid-scale models, Comput. Fluids 59, 101 (2012).